DEVELOPMENT OF A DYNAMIC MODEL FOR A MANGANESE OXYGEN REFINING (MOR) CONVERTER

J. Nell and I. Nolet

Hatch Africa, Private Bag X20, Gallo Manor, 2052 SOUTH AFRICA,
Johannes.nell@hatch.co.za, inolet@hatch.com.au

ABSTRACT

A typical Manganese Oxygen Refining (MOR) process involves the injection of inert gases through bottom tuyeres and top lance injection of oxygen to de-carburise a charge of HC FeMn, containing about 7%C, down to a carbon content of 1.5-2%C. The melt temperature typically needs to be controlled below 1750^{o}C to protect vessel refractories, and to minimise Mn losses to the gas phase. Fluxes can be added to adjust slag chemistry.

In order to study optimal process conditions, a dynamic model of this process, incorporating kinetic and thermodynamic aspects, has been developed using Metsim™. Non-ideal solution models have been incorporated for the metal and slag phases. The bubble interface is modelled using a Free Energy Minimiser (FEM) to which a metal and slag flow is directed, thereby controlling mass transfer between the reaction site and each of the bulk phases. Logic controllers have been included to modify top and bottom blowing rates based on blowing time and trigger/stop material additions based on totalising instruments and time of the cycle.

The main input values and other tuning parameters can be readily modified by the user via a user-friendly Excel interface handling the simulation input and results. A large number of user-created objects facilitate model input management from the interface.

Examples are presented to demonstrate the model behaviour for changes in process conditions such as metal fines addition, slag chemistry and top blowing rate.

1 INTRODUCTION

Hatch developed a dynamic process model of a typical MOR converter to run various cases with the objective to study parameters such as temperature control, slag/refractory interaction and Mn recovery.

The model incorporates a dynamic (transient) feature, mass and energy balance capabilities, calculation of equilibrium conditions (using a Free Energy Minimiser) and mass transfer aspects in the metal and slag phases. Once validated and calibrated, such a model can be successfully used for predictive purposes and evaluate various process conditions and their impact on metallurgical performance (such as slag make, Mn losses to slag, Mn losses to vapour, slag-refractory interactions, etc.) This paper describes the development of the dynamic Metsim™ model in details and explores model behaviour and sensitivity for various process conditions.

In future, this model will be further developed, validated and calibrated against operational data as it could become a useful process control and simulation tool for the metallurgist.

2 DYNAMIC MODEL DEVELOPMENT

Metsim™ has been selected as the modeling platform. This software is widely used for metallurgical mass and energy balances, but not extensively used for thermodynamic modeling. This is due to the fact that the Metsim™ Free Energy Minimiser (FEM) is based on ideal solution models by default (i.e. $a_i=X_i$ or $\gamma_i=1$). The software however offers the possibility to program customized relationships for γ_i's. This type of modeling has been done before in Metsim™ for the simulation of a HC FeMn furnace by

Li, Morris & Robertson [Ref.1] as well as for a FeCr converter by Booysen et al. [Ref.2]. A more simplistic approach was used to construct the model for the MOR process by not using transitory reaction interfaces (representing different heights in the metal bath). It would be possible to add transitory reaction interfaces to the model if more substantial operating data was available to validate the more complex model. The current structure of the MOR process model is shown in Figure 1.

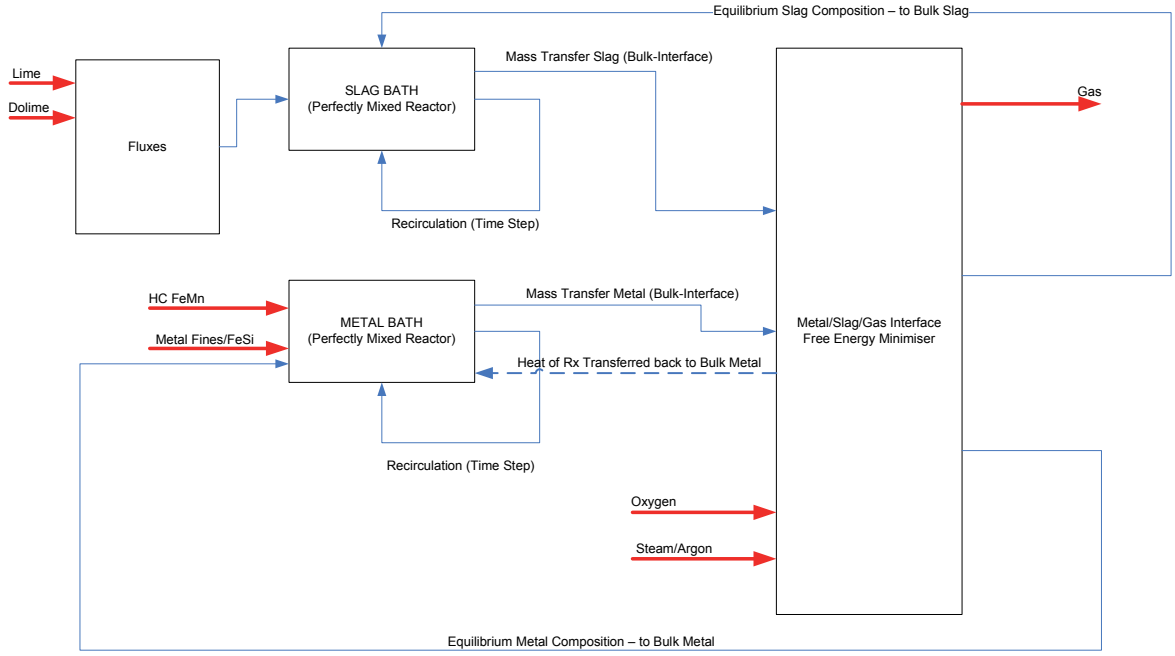

Figure 1: Structure of the MOR Process Metsim™ Model

The model incorporates a bulk metal phase and a bulk slag phase, both represented as perfectly mixed reactors. A calculated mass flowrate of metal and slag are directed to a reaction interface (the Free Energy Minimiser) where equilibrium conditions are calculated. The equilibrium metal and slag are sent back to their respective bulk phases, where the new mass and composition of the bulk phases are calculated. The top and bottom blowing gases are supplied to the reaction interface for reaction. The model also incorporates a flux addition unit operation, in which various material additions can be made throughout the cycle. The model is run for a pre-determined number of time steps: all equilibrium conditions and phase quantities, temperatures and compositions are calculated at each time step.

2.1 Thermodynamic Models for Metal and Slag Phases

The initial Unified Interaction Parameter Model (UIPM) has been widely used for estimating activities of components in molten iron, but the parameters are not applicable to ferromanganese alloys. Li and Morris [Ref.1] subsequently developed a set of UIPM parameters for FeMn alloys and Li, Morris & Robertson [Ref.2] also made use of these UIPM parameters in the Metsim™ modeling of a HC FeMn furnace.

The UIPM parameters developed by Li & Morris [Ref.1] were therefore programmed into the Metsim™ model for the metal phase component activity coefficients. These parameters are shown in Equations [1] to [14].

$$\varepsilon_{Fe-C} = \frac{2510}{T} \quad [1]$$

$$\varepsilon_{Fe-Si} = \frac{4180}{T} \quad [2]$$

$$\varepsilon_{C-C} = \frac{-7530}{T} \quad [3]$$

$$\varepsilon_{C-Si} = \frac{20750}{T} \quad [4]$$

$$\varepsilon_{Si-Si} = \frac{25930}{T} \quad [5]$$

$$\varepsilon_{Fe-C-C} = \frac{4180}{T} \quad [6]$$

$$\varepsilon_{C-C-C} = \frac{97880}{T} \quad [7]$$

$$\varepsilon_{C-C-Si} = \frac{46000}{T} \quad [8]$$

$$\varepsilon_{Si-Si-Si} = \frac{4500}{T} \quad [9]$$

$$\ln \gamma_C^0 = -4.25 + \frac{5200}{T} \quad [10]$$

$$\ln \gamma_{Si}^0 = \frac{-12680}{T} \quad [11]$$

$$\ln \gamma_{Mn} = \frac{1}{2}\left[2\varepsilon_{FeC}X_{Fe}X_C + \varepsilon_{CC}X_C^2 + 2\varepsilon_{FeSi}X_C X_{Si} + \varepsilon_{SiSi}X_{Si}^2\right] - \frac{2}{3}\left[3\varepsilon_{FeCC}X_{Fe}X_C^2 + \varepsilon_{CCC}X_C^3 + 3\varepsilon_{CCSi}X_C^2 X_{Si} + \varepsilon_{SiSiSi}X_{Si}^3\right] \quad [12]$$

$$\ln \gamma_{Si} = \ln \gamma_{Si}^0 + \ln \gamma_{Mn} + \varepsilon_{FeSi}X_{Fe} + \varepsilon_{CSi}X_C + \varepsilon_{SiSi}X_{Si} + \varepsilon_{CCSi}X_C^2 + \varepsilon_{SiSiSi}X_{Si}^2 \quad [13]$$

$$\ln \gamma_C = \ln \gamma_C^0 + \ln \gamma_{Mn} + \varepsilon_{FeC}X_{Fe} + \varepsilon_{CC}X_C + \varepsilon_{CSi}X_{Si} + 2\varepsilon_{FeCC}X_{Fe}X_C + 2\varepsilon_{CCSi}X_{Si}X_C + \varepsilon_{CCC}X_C^2 \quad [14]$$

where: T is the temperature in Kelvin
X is the molar fraction of the component in the metal phase

In addition, constant activity coefficients were incorporated for dissolved species ([N] and [H]) in the metal. In the absence of data for FeMn alloys, data for solubility in pure Fe was used. For this model, activity coefficients for dissolved hydrogen and dissolved nitrogen were included.

For the slag phase, customized activity coefficient expressions were derived and incorporated to the model. Based on the study done by Eric & Cenzigler [Ref.3], it was found that the activity of MnO was a strong function of slag basicity. FactSage™ calculations were performed in the MnO-CaO-MgO-SiO_2-Al_2O_3 system for a range of slag compositions and temperatures. Correlations between activity coefficients (for SiO_2, MgO, CaO and MnO) and slag basicity were obtained for various temperatures. To avoid instabilities and convergence issues when running the dynamic model, γ_i's were assumed to be independent of temperature between 1600°C and 1750°C. Best-fit equations [15] to [18] were developed for T=1600°C and were incorporated in the Metsim™ model:

$$\gamma_{SiO2} = 0.0102B^2 - 0.0441B + 0.0525 \quad [15]$$

$$\gamma_{MgO} = 0.7606B - 0.4225 \quad [16]$$

$$\gamma_{MnO} = 1.1229B + 0.1901 \quad [17]$$

$$\gamma_{CaO} = 0.2215B^2 - 0.7019B + 0.6078 \quad [18]$$

Where: B is slag basicity defined as: $$B = \frac{(wt\%CaO + wt\%MgO)}{wt\%SiO_2} \quad [19]$$

Based on FactSage™ results for a range of slag compositions and temperatures, the following activity coefficients were assumed constant:

$$\gamma_{Al_2O_3} = 0.006 \quad [20]$$

$$\gamma_{FeO} = 2.0 \quad [21]$$

2.2 Mass Transfer Rates to the Reaction Interface

To obtain a realistic decarburization rate, kinetics must be taken into account by setting mass transfer rates for the bulk metal and bulk slag to the reaction interface. The generic mass transfer equation used is shown in Equation [19]:

$$W = k \cdot A \cdot \rho \cdot (w_{eq} - w_{bulk}) \quad [22]$$

Where:

W is the rate of transfer of a species into the phase (kg/s)
k is the mass transfer coefficient (m/s)
A is the surface area for reaction (m^2)
ρ is the density of the phase (kg/m^3)
w_{eq} is the mass fraction of a species at equilibrium
w_{bulk} is the mass fraction of a species in the bulk phase

Literature data on the metal mass transfer coefficient show values between 10^{-4} and 10^{-3} $m.s^{-1}$. An average value of 0.0005 m/s was assumed in this model. This is consistent with the value used by Roy & Robertson [Ref.4] in their mathematical modelling of an AOD vessel for stainless steel making and the value used by Booysen et al. [Ref.5] in their modelling of an intermediate carbon charge chromium CLU converter.

The density of the alloy was taken as 7200 kg/m^3 and that of slag as 3500 kg/m^3.

The surface area of reaction A (in equation 22) is difficult to determine because it depends on the number and size distribution of gas bubbles. The surface area was therefore determined by calibration with the known decarburization time in the converter vessel. The mass transfer rate of the metal to the interface was estimated to be 1.6 tonnes per minute (tpm), hence corresponding to a surface area for reaction of 7.4 m^2. Because of the variability of the slag mass in the system during the cycle, the proportion of slag sent to the interface was varied in proportion to the slag volume.

2.3 User-Created Objects and Logic Controllers

For ease of use, a number of user-created objects were generated in Metsim™. The values assigned to these variables can be modified via the Excel interface at certain points in time with the help of logic controllers. Examples of user-created objects are shown in Table 1.

Table 1: Some Examples of User-Created Objects in Metsim™

User-Created Object	Units	Description
USO2Flowrate	Nm^3/h	Oxygen Flowrate
USFlowSteam	Nm^3/h	Bottom Steam Blowing Rate
USFlowArgon	Nm^3/h	Bottom Argon Blowing Rate
USTargetSlagBasicity	-	Targeted Slag Basicity
USReducedOxygen	Nm^3/h	Reduced Top Lance Oxygen Flowrate

Logic controllers were created to modify the values of specific variables at a specific time during the cycle. Controllers can be generated to make material additions (such as fluxes and metal fines), or modify the blowing sequence. Examples of logic controllers are given in Table 2. The logic controllers can be modified to suit the true decision-making process followed by the operator during the converter cycle.

Table 2: Examples of Logic Controllers in Metsim™

Controller Action	Condition to be met
Blow oxygen at 20 Nm^3/min for 14 minutes	Stop at t=15 minutes
Blow oxygen at 6 Nm^3/min for 6 minutes	Start at t=15 minutes and Stop at t=21 minutes
Blow steam at 7.5 Nm^3/min for 6 minutes	Start at 5=15 minutes and stop at t=21 minutes
Add 130kg of FeSi 75	At t=22 minutes
Add 130kg of lime	At t=22 minutes
Stop addition of FeSi 75	Once FeSi totaliser has reached 130kg
Stop addition of lime	Once lime totaliser has reached 130kg

2.4 Vessel Heat Losses

Converter heat losses have been estimated on the basis of conductive losses through a typical MgO-C lining and safety lining and radiation losses through the converter mouth. The conductive heat losses were estimated with Fourier's law of conduction:

$$q = \frac{A \cdot (T_{hot} - T_{cold})}{\frac{x_1}{k_1} + \frac{x_2}{k_2} + \frac{x_3}{k_3}}, \qquad [23]$$

where:
q is the heat transferred per unit time (W)
A is the conductive area (m^2)
T_{hot} is the temperature at the hot face (K)
T_{cold} is the temperature at the cold face (K)
x is the thickness of a particular layer (m)
k is the thermal conductivity of a particular layer (W/m.K)

For simplification purposes, a constant hot face temperature of T=1600°C was used. For radiation losses, the Stefan-Boltzmann Law for gray bodies was used:

$$q = \varepsilon \cdot \sigma \cdot A \cdot T^4, \qquad [24]$$

where:
q is the heat transferred per unit time (W)
ε is the emissivity of the bath (assumed at 0.4[1])
σ is Stefan-Boltzmann's constant ($W/m^2/K^4$)
A is the area of the emitting body (m^2)
T is the absolute temperature of the emitting body (K)

The total heat loss (by conduction and radiation) was incorporated into the Metsim™ model and can readily be changed using the Excel interface.

[1] Emissivity reported for a molten steel bath by Nippon Steel [Ref.6]

3 MODEL VALIDATION

To validate the model behaviour, the model was calibrated against data published in Patent 79/0169 “Process for Decarburising Ferro-Manganese”. In this patent, a small 6t converter is charged with HC FeMn and dolomite. Oxygen is blown at full rate for 14 minutes, then together with steam at a reduced flowrate for 6 minutes. FeSi and lime are then added to the melt to reduce MnO losses to slag with a soft argon blow for 5 minutes. Alloy and slag tonnages and compositions obtained are published and can be used to validate the Metsim™ model. Model results were compared to key performance indicators published in the patent, as shown in Table 3.

Table 3: Model Validation against Published Data

Parameter	Units	Data Published in Patent 79/0169	Metsim Model Output
Final Metal Mass	tonnes	4.77	4.75
Final Metal Composition	wt%	81.0%Mn 1.33%C 0.77%Si	80.5%Mn 1.2%C 0.8%Si
Final Slag Mass	kg	581	586
Final Slag Composition	wt%	30%MnO 27%SiO_2 32%CaO <1%Al_2O_3	35%MnO 26%SiO_2 32%CaO <1%Al_2O_3

It is important to note that the model parameters have to be adjusted for specific operating conditions occurring in the vessel under study. For example, operating in a different slag basicity regime brings about the need for a different thermodynamic model for the slag phase components.

4 EXAMPLES OF MODEL BEHAVIOUR

Figures 2 and 3 present examples of graphic Metsim™ outputs for some of the key parameters during the converter cycle, including: bulk metal temperature, metal and slag mass and alloy composition over time.

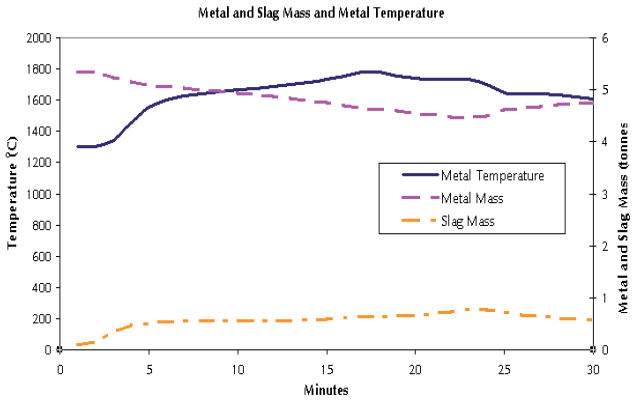

Figure 2: Bulk metal temperature, metal and slag mass

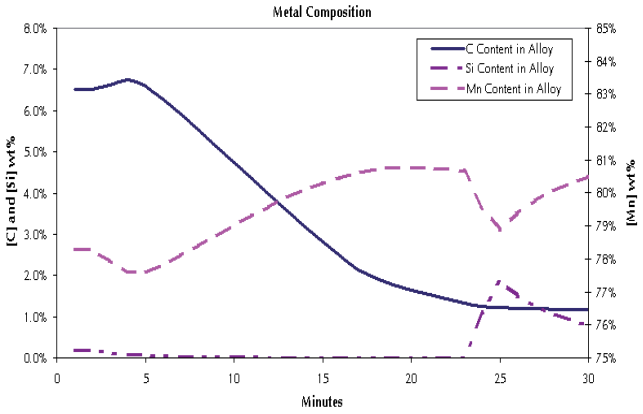

Figure 3: Bulk metal carbon content, Si content and Mn content during converter cycle

With the calibrated model, various example case studies were run to analyse the impact of various process parameters on converter performance:

- Base Case: Steam bottom-blowing, top blowing rate of 20 Nm^3/min, slag basicity of 1.6
- Case A: Add 500kg of metal fines
- Case B: Slag basicity of 1.2 instead of 1.6, to demonstrate the impact of slag chemistry on MnO reduction efficiency
- Case C: Top blowing rate of 30 Nm^3/min instead of 20 Nm^3/min, to demonstrate the impact of blowing rate on Mn losses.

Some of the key performance indicators for each of these case studies are presented in Table 4.

Table 4: Summary of Key Results for Cases A, B and C

Parameter	Units	Base Case	Case A	Case B	Case C
Top Oxygen Blowing Rate	Nm^3/min	20/6/0	20/6/0	20/6/0	30/6/0
Final Slag Basicity	-	1.6	1.6	1.2	1.6
Metal Fines Addition	kg	0	500	0	0
Blowing Time	min	14/6/5	14/6/5	14/6/10	11/6/5
Final Alloy Mass	tonnes	4.75	5.24	4.85	4.69
Final Slag Mass	kg	586	596	534	584
Final Slag MnO Content	wt% MnO	36	37	22	37
Final Bulk Metal Temperature	^oC	1609	1479	1531	1609
Mn losses to slag	tonnes	0.2	0.2	0.1	0.2
Mn losses to gas	tonnes	0.2	0.2	0.2	0.3

Figures 4 to 7 demonstrate variations of the CO/CO_2 ratio at the reaction interface, bulk metal carbon content, bulk slag MnO content and bulk metal temperature as a function of time for the various cases.

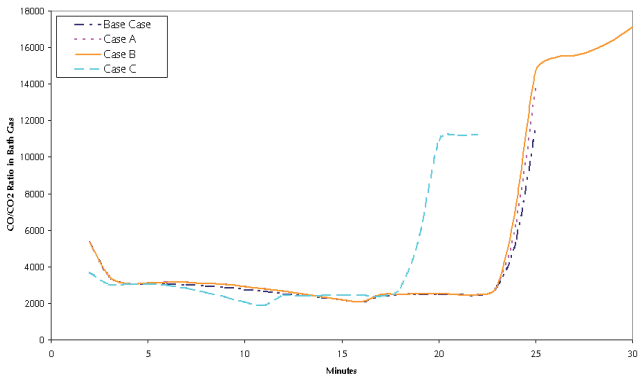

Figure 4: Variation of CO/CO_2 Ratio at reaction interface as a function of time for various cases

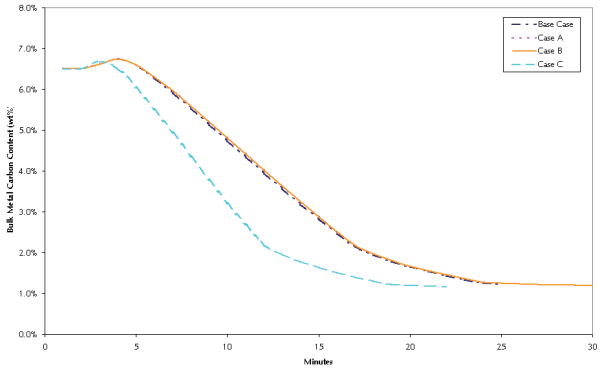

Figure 5: Variation of bulk metal carbon content as a function of time for various cases

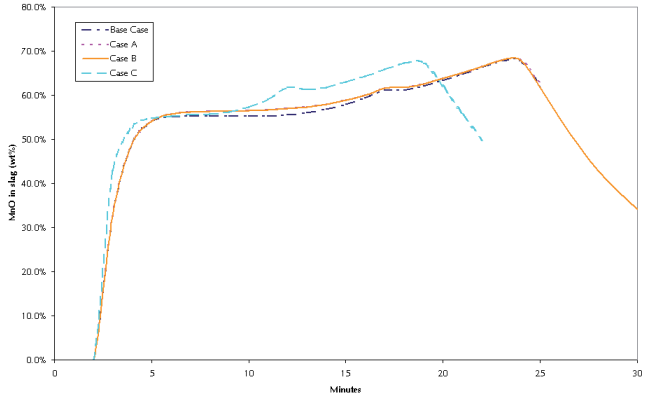

Figure 6: Variation of bulk slag MnO content as a function of time for various cases

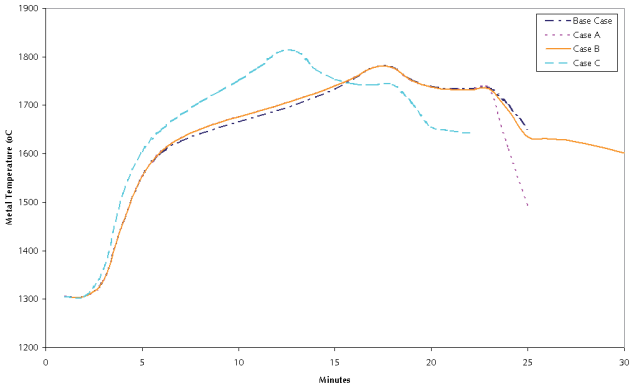

Figure 7: Variation of bulk metal temperature as a function of time for various cases

In Case A, it is interesting to note the chilling effect caused by the addition of 500 kg of metal fines to the bath. Figure 7 demonstrates the drop in metal temperature, and by thermal equilibrium, a drop in slag temperature is also experienced. It is important to choose carefully when to perform such an addition during the cycle as well as the quantity to be added, so as to remain above the slag liquidus temperature and avoid operating with a "dry" slag. In Case A, the slag liquidus temperature is estimated at 1785^{o}C. At the final bath temperature of 1479^{o}C, approximately 60% of the slag is liquid and comprises a significant quantity of solids (mostly MnO-MgO monoxide and Ca_2SiO_4) that could potentially impact skimming and tapping operations.

In Case B, a lower slag basicity was investigated by simply adding more FeSi to increase the final slag SiO_2 content. Due to the higher extent of reduction achieved with the additional FeSi, this results in a lower slag make at a lower MnO content (Fifure 6). Even though this may seem advantageous, it is essential to assess other metallurgical aspects before contemplating such a strategy. Operating at a basicity of 1.2 (instead of 1.6) is a completely different regime of operation, as the slag liquidus temperature decreases significantly from approximately 1785^{o}C to 1340^{o}C. At the converter operating temperature, the slag is hence 100% liquid and in the absence of solid phases, slag MgO saturation must be assessed for refractory protection.

Table 5: Slag MgO Saturation Assessment (Base Case vs. Case B)

	Units	Base Case	Case B
MnO	wt%	35.9	21.9
SiO_2	wt%	25.5	35.7
MgO	wt%	6.8	7.4
CaO	wt%	31.6	34.7
Liquidus Temperature	^{o}C	1785	1340
Final Temperature	^{o}C	1609	1531
% liquid slag at T_{final}	%	85	100
MgO Saturation at T_{final}	wt%	5	13.5
Saturation?	-	Yes	No

Table 5 demonstrates that the strategy followed in Case B, whereby the quantity of FeSi was simply increased, is not recommended as it leads to under-saturation conditions in the slag. Calculations using FactSage™ show that a MgO level of approximately 13.5 wt% would be required for saturation (instead of 7.4 wt%). The fluxing regime would therefore also have to be modified to operate at a basicity of 1.2, in which the proportion of dolomite should be increased to ensure slag MgO saturation and refractory protection.

In Case C, increasing the top lance blowing rate from 20 Nm^3/min to 30 Nm^3/min results in a lower blowing time of 11 minutes (vs. 14 minutes). The faster decarburisation is shown in Figure 5 and the associated faster temperature rise is shown in Figure 7. The faster temperature rise results in higher Mn losses to the gas phase (0.3 tonnes vs. 0.2 tonnes), lowering the overall Mn recovery. Productivity can therefore be increased at the price of Mn recovery. Depending on the converter vessel and the company's operating philosophy, it is essential to find the optimal blowing rate from an economic perspective – minimising converter cycle time or maximising Mn recovery.

5 CONCLUSIONS

A dynamic model of the MOR process, incorporating kinetic and thermodynamic aspects, has been developed using Metsim™. Non-ideal solution models have been incorporated for the metal and slag phases. The bubble interface is modelled using a Free Energy Minimiser (FEM) to which a metal and slag flow is directed, thereby controlling mass transfer between the reaction site and each of the bulk phases. Logic controllers were included to make material additions or modify the blowing recipe upon certain conditions.

The main input values and other tuning parameters can be readily modified by the user via a user-friendly Excel interface handling the simulation input and results. A large number of user-created objects facilitate model input management from the interface.

The model was validated and calibrated against published data for Patent 79/0169 and was thereafter used for predictive purposes in various case studies. These case studies demonstrated the impact of metal fines addition, lower slag basicity and increased top lance blowing rate. The Metsim™ model can be customized for most top-blown bottom-stirred FeMn converting operations. The blowing gas can be readily modified and the logic controllers can be programmed to suit the decision-making process by the operator during the converter cycle.

In future, this model will be further developed, validated and calibrated against operational data as it could become a useful process control and simulation tool for the metallurgist.

6 ACKNOWLEDGEMENTS

The authors would like to thank Prof. David Robertson from the University of Missouri-Rolla for his great advice and contribution to the development of this model.

7 REFERENCES

[1] Li, H., Morris, A.E. and Robertson, D.G.C., “Thermodynamic Model for MnO-Containing Slags and Gas-Slag-Metal Equilibrium in Ferromanganese Smelting”, Metallurgical and Materials Transactions B, Volume 29B, Dec.1998, pp. 1181-1191.

[2] Li, H., Morris, A.E. and Robertson, D.G.C., “The Development of a Multi-stage Model for a Ferromanganese Furnace and Simulation Resutls”, Electric Furnace Conference Proceedings, 1996, pp. 227-235

[3] Cengizler, H., Eric, R.H., “Activity of MnO in MnO-CaO-MgO-SiO_2-Al_2O_3 Slags at 1500^oC”, Steel Research Intl, Vol. 77, No.1, 2006, pp.793-802

[4] Roy, T.D., Robertson, D.G.C., “Mathematical Model for Stainless Steelmaking: Part 1 Argon-Oxygen and Argon-Oxygen-Steam Mixtures”, Ironmaking and Steelmaking, No.5, 1978, pp.198-206.

[5] Booysen, L.M., Nelson, L.R., Swamy, K.N., Visser, M., “Development of an Operator Guidance System for Intermediate Carbon Charge Chromium Production”, Infacon 2004.

[6] Sugiura, M., Nakao, R., Nagata, S., Tsubota, E., Yamazaki, T., Tanaka, T., Kumazawa, H., Nagai, W., “Development of New Technique for Continuous Molten Steel Temperature Measurement”, Nippon Steel Technical Report No.89, 2004, pp.23-27.